Physics Letters B 719 (2013) 362–366

Contents lists available at SciVerse ScienceDirect

Physics Letters B

www.elsevier.com/locate/physletb

Charge radii of odd-A $^{191-211}$Po isotopes

M.D. Seliverstov [a,b,c,d,e,f,*], T.E. Cocolios [a,g], W. Dexters [a], A.N. Andreyev [a,d,e,f], S. Antalic [h], A.E. Barzakh [b], B. Bastin [a,1], J. Büscher [a], I.G. Darby [a], D.V. Fedorov [b], V.N. Fedoseyev [g], K.T. Flanagan [i,j], S. Franchoo [k], S. Fritzsche [l,m], G. Huber [c], M. Huyse [a], M. Keupers [a], U. Köster [n], Yu. Kudryavtsev [a], B.A. Marsh [g], P.L. Molkanov [b], R.D. Page [o], A.M. Sjødin [g,p,1], I. Stefan [k], J. Van de Walle [a,g,2], P. Van Duppen [a,g], M. Venhart [a,q], S.G. Zemlyanoy [r]

[a] Instituut voor Kern- en Stralingsfysica, KU Leuven, B-3001 Leuven, Belgium
[b] Petersburg Nuclear Physics Institute, NRC Kurchatov Institute, 188300 Gatchina, Russia
[c] Institut für Physik, Johannes Gutenberg Universität, D-55099 Mainz, Germany
[d] School of Engineering and Science, University of West Scotland, PA1 2BE Paisley, United Kingdom
[e] Scottish Universities Physics Alliance (SUPA), United Kingdom
[f] Department of Physics, University of York, York, YO10 5DD, United Kingdom
[g] CERN, CH-1211 Geneva 23, Switzerland
[h] Department of Physics and Biophysics, Comenius University, 842 48 Bratislava, Slovakia
[i] Department of Physics, University of Manchester, M60 1AD Manchester, United Kingdom
[j] Centre de Spectrométrie Nucléaire et de Spectrométrie de Masse, F-91405 Orsay, France
[k] Institut de Physique Nucléaire, F-91406 Orsay, France
[l] GSI Helmholtzzentrum für Schwerionenforschung, D-64291 Darmstadt, Germany
[m] Department of Physics, University of Oulu, P.O. Box 3000, Fin-90014, Finland
[n] Institut Laue-Langevin, F-38042 Grenoble, France
[o] Oliver Lodge Laboratory, University of Liverpool, L69 7ZE Liverpool, United Kingdom
[p] KTH-Royal Institute of Technology, SE-10044 Stockholm, Sweden
[q] Institute of Physics, Slovak Academy of Sciences, 845 11 Bratislava, Slovakia
[r] Joint Institute of Nuclear Research, 141980 Dubna, Moscow Region, Russia

ARTICLE INFO

Article history:
Received 26 September 2012
Received in revised form 16 January 2013
Accepted 20 January 2013
Available online 29 January 2013
Editor: V. Metag

Keywords:
Isotope shift
Nuclear charge radius
Shape coexistence

ABSTRACT

Isotope shifts have been measured for the odd-A polonium isotopes $^{191-211}$Po and changes in the nuclear mean square charge radii $\delta\langle r^2\rangle$ have been deduced. The measurements were performed at CERN-ISOLDE using the in-source resonance-ionization spectroscopy technique. The combined analysis of these data and our recent results for even-A polonium isotopes indicates an onset of deformation already at ^{197,198}Po, when going away from stability. This is significantly earlier than was suggested by previous theoretical and experimental studies of the polonium isotopes. Moreover and in contrast to the mercury isotopes, where a strong odd–even staggering of the charge radii of the ground states was observed by approaching the neutron mid-shell at $N = 104$, no such effect is present in polonium down to ^{191}Po. Consequently the charge radii of both isomeric and ground states of the odd-A polonium isotopes follow the same trend as the even-A isotopes.

Shape coexistence at low-excitation energy in nuclei is a phenomenon for which interest has been continuously growing on both the experimental and theoretical fronts [1–5]. Studies of the polonium isotopes ($Z = 84$) are required to understand the transition across the proton shell closure at $Z = 82$. Earlier theoretical studies which used both macroscopic–microscopic approaches (*e.g.* [6–9]) and self-consistent Hartree–Fock–Bogoliubov calculations (*e.g.* [10,11]) have predicted that, while the heavier $^{194-210}$Po isotopes should remain nearly spherical in their ground states, a sudden onset of oblate deformation with $\beta_2 \sim -0.20$ is expected around ^{192}Po. Furthermore, an equally abrupt transition to a prolate ground state with $\beta_2 = 0.3$ (see *e.g.* Refs. [7]) is expected for the lighter even-A polonium isotopes. These expectations were confirmed by a large number of recent α-, β- and γ-spectroscopy studies [12–15], which probed both the ground state (via particle decay) and low-lying excited configurations. Indeed, several experimental studies have concluded that while the ground state

* Corresponding author at: Instituut voor Kern- en Stralingsfysica, KU Leuven, B-3001 Leuven, Belgium.
E-mail address: Maxim.Seliverstov@cern.ch (M.D. Seliverstov).
[1] Present address: GANIL, France.
[2] Present address: IBA, Belgium.

0370-2693
http://dx.doi.org/10.1016/j.physletb.2013.01.043

has a spherical shape near the closed neutron shell $N = 126$, an excited presumably oblate deformed configuration sharply lowers its energy in the neutron-deficient polonium isotopes [16–18]. This leads to a strong spherical-oblate mixing at low excitation energy in ^{194}Po [15,19,20], with ^{192}Po being the first neutron-deficient polonium isotope where the oblate deformed configuration becomes the dominant component in the ground state, as observed both by in-beam γ-ray spectroscopy [12] and α-decay studies [13]. In ^{191}Po, it was deduced from the large hindrance in the α-decay that the high-spin isomer is deformed and possesses a significant, presumably oblate, intruder component while the low-spin isomer remains weakly deformed [18]. In ^{190}Po, studied initially via α-decay [3] first evidence for a presumably prolate intruder component in its ground state was suggested. This inference was recently confirmed by an in-beam study [21], which identified a low-lying prolate band in this nucleus. Finally, recent α-decay studies of ^{187,188}Po provided evidence for a prolate-deformed configuration of their ground states [13,22].

These observations should be directly reflected in the ground state properties such as charge radii, which can be investigated by means of laser spectroscopy in a nuclear-model-independent way. Prior to our work, laser spectroscopic studies were limited to the long-lived nuclides $^{200,202,204-210}$Po [23] only. Recent developments in the highly sensitive in-source laser-photoionization spectroscopy technique [24,25] combined with the increased accuracy of atomic calculations for heavier elements, enables the extension of these measurements towards more exotic nuclei.

In our recent work [26] the charge radii for even-A $^{192-210,216,218}$Po were reported. In the present Letter we discuss the results of the charge radii measurements for the neighbouring odd-A polonium isotopes obtained during the same experimental campaign. From the combined analysis of our data for the even-A and odd-A polonium isotopes we conclude that, when going away from the $N = 126$ closed shell towards the neutron-deficient isotopes, an onset of deformation occurs at ^{197,198}Po, which is significantly earlier than has been indicated by previous experimental and theoretical studies.

The experiments were performed at the ISOLDE facility [27]. Beams of $^{193-199}$Po were produced in the first experimental campaign (Run I, 2007) and beams of $^{191-195,201,203,209,211}$Po were produced in the second campaign (Run II, 2009). The polonium nuclei were produced in spallation reactions induced by the 1.4 GeV proton beam (intensity up to 2 μA) from the CERN PS Booster impinging on a UC_x target (50 g/cm^2 of ^{238}U). The spallation products diffused out of the high temperature target ($T \approx 2050\,^\circ$C) and effused as neutral atoms into the cavity of the Resonance Ionization Laser Ion Source, RILIS [28]. The polonium atoms are resonantly ionized within this cavity when the laser beams were frequency tuned to the three-step polonium ionization scheme (see Fig. 1).

Laser light for the resonant excitation of the first two atomic transitions was provided by two tunable pulsed dye lasers. The ultraviolet radiation was obtained by tripling the frequency of the fundamental dye laser radiation using BBO crystals. Copper vapour lasers (CVL) operating at a pulse repetition rate of 11 kHz (Run I) and a Nd:YAG laser operating at 10 kHz (Run II) were used to pump the dye lasers and to perform the excitation from the second excited state into the continuum (the third step). The use of a single powerful Nd:YAG laser (total power of 100 W) instead of the copper vapour oscillator-amplifier laser system provided better photoionization stability.

For the atomic-spectroscopy measurements, a narrow linewidth laser (1.2 GHz) was used for the second excitation step, while the laser linewidth for the first step laser was more than 20 GHz. Whilst counting the mass separated photoions, the frequency ν_L of the second step laser was scanned. The laser power for the second excitation step was reduced to avoid line broadening caused by saturation.

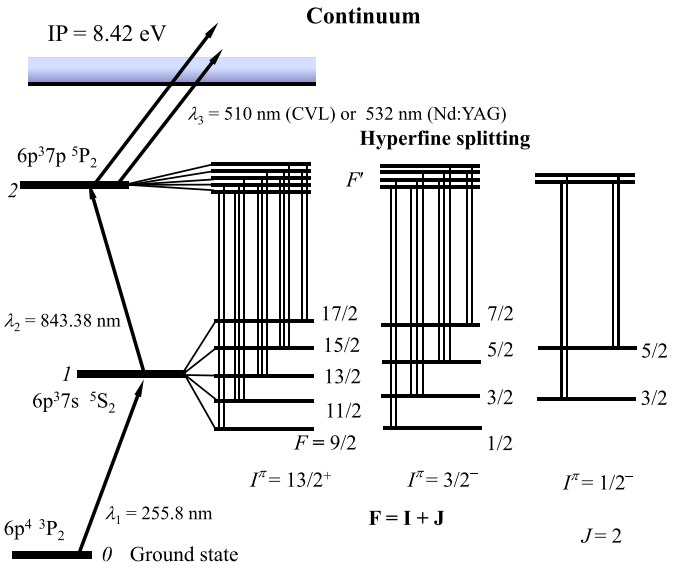

Fig. 1. The three-step laser-ionization scheme for polonium [29]. The electronic configurations for the levels involved and the laser wavelengths for each step are shown. The hyperfine structures for the $13/2^+$, $3/2^-$ and $1/2^+$ states of odd-A polonium isotopes are shown schematically (not on scale). The hyperfine lines expected for $I = 13/2$ (five groups), $I = 3/2$ (four groups) and $I = 1/2$ (two groups) are also shown.

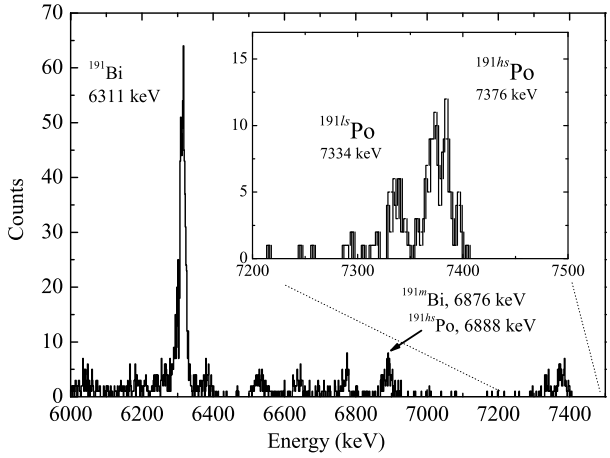

Fig. 2. The α-decay spectrum accumulated at $A = 191$ while scanning the laser frequency through the resonance region. The inset shows an enlargement of the spectrum around the two α-lines of ^{191}Po (low-spin (*ls*) and high-spin (*hs*) isomers).

The short-lived α-decaying isotopes $^{191-197,211}$Po were implanted and detected via their characteristic α-decay at the windmill system, a rotary sample holder hosting ten thin carbon foils (20 μg/cm^2) in front of a Si detector (described in Ref. [30]). The dominantly β-decaying isotopes $^{199-203}$Po were detected via their β-decay and the subsequent characteristic γ-ray emission at the ISOLDE tape station. The decays of the ground and isomeric states of polonium isotopes could be clearly distinguished based on the difference in their α-particle or γ-ray energies down to the extremely exotic ^{191}Po isotope produced with a yield of ~ 0.01 ions/s (see Fig. 2).

The higher yield for longer-lived ^{209}Po enabled it to be measured directly in a Faraday cup. More experimental details are given in Refs. [26,31]. The optical spectra obtained are shown in Figs. 3 and 4. The atomic spectroscopic measurements were

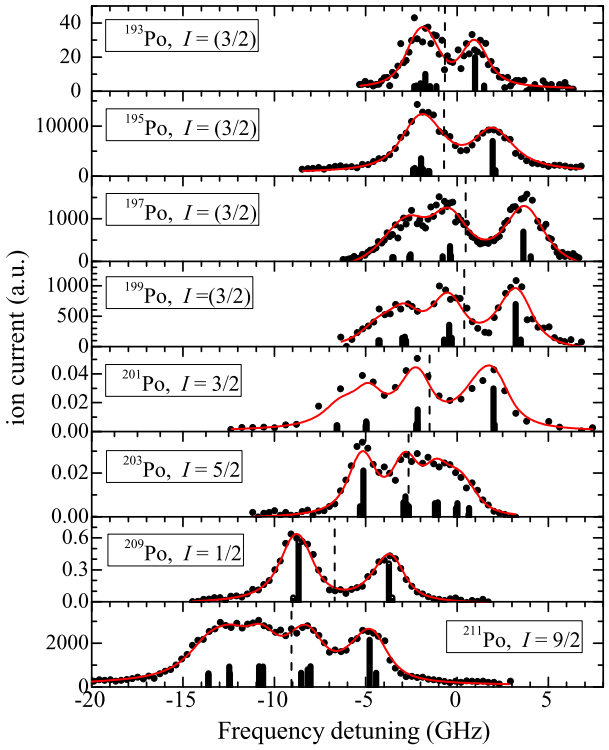

Fig. 3. Typical examples of the optical spectra of ground and low-spin states of polonium isotopes collected in individual scans. Here the dependence of the number of the detected photoions (deduced from the number of α-particle or γ-rays) on the laser frequency detuning is shown. Frequency detuning is shown with respect to the resonance frequency of ^{196}Po. Solid lines represent a fit to the data (see text). The calculated positions and relative intensities of the individual hyperfine components are also shown with vertical bars, the positions of the hfs centroids (ν_0) are shown with vertical dashed lines.

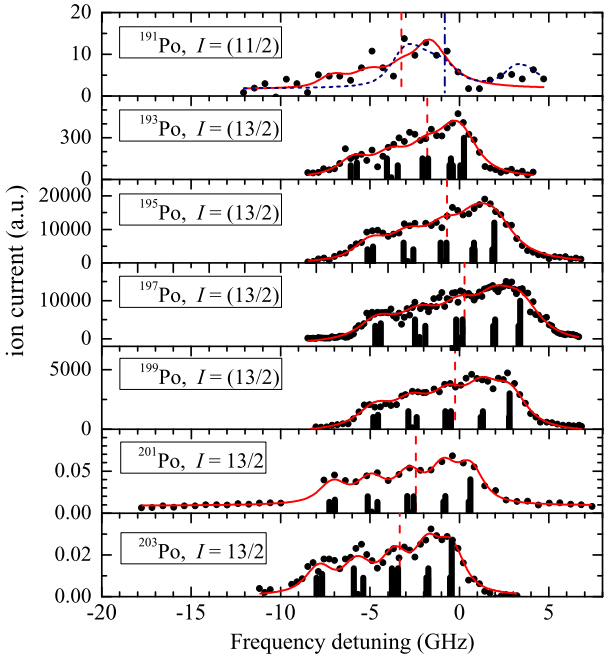

Fig. 4. The same as Fig. 3, but for the high-spin states. For ^{191}Po the combined statistics obtained during the scans is displayed. For ^{191}Po the fits with $B > 0$ and $B < 0$ are shown by the solid and dashed lines, respectively.

Table 1
Measured values of the isotope shifts $\delta\nu$, deduced values of the mean-square charge radii changes $\delta\langle r^2\rangle$ and estimation of the deformation parameter β_2 based on the charge radii. The spin assignments of the isomer and ground states in $^{191-199}$Po isotopes could not be determined in this work, hence shown in brackets in the table and Figs. 3 and 4. They are based on the systematics of allowed α-decay to the states in the corresponding lead daughter isotopes, for which spins have been determined.

Isotope	I^π	$\delta\nu_{A,196}$ (GHz)	$\delta\langle r^2\rangle_{A,210}$[a] (fm^2)	$\langle\beta_2^2\rangle^{1/2}$
^{191hs}Po	$(11/2^+ - 15/2^+)$[b]	−3.24(45)[c]	−0.350(40)[c]	0.27
^{191hs}Po	$(11/2^+ - 15/2^+)$[b]	−0.82(45)[d]	−0.553(40)[d]	0.23
^{193ls}Po	$(3/2^-)$	−0.59(15)	−0.576(13)	0.21
^{193hs}Po	$(13/2^+)$	−1.11(15)	−0.532(13)	0.22
^{195ls}Po	$(3/2^-)$	−0.29(15)	−0.604(13)	0.18
^{195hs}Po	$(13/2^+)$	−0.61(15)	−0.575(13)	0.18
^{197}Po	$(3/2^-)$	0.30(15)	−0.657(13)	0.13
^{197m}Po	$(13/2^+)$	0.12(15)	−0.642(13)	0.13
^{199}Po	$(3/2^-)$	0.11(15)	−0.644(13)	0.09
^{199m}Po	$(13/2^+)$	−0.72(15)	−0.574(13)	0.12
^{201}Po	$3/2^-$	−1.51(15)	−0.510(13)	0.10
^{201m}Po	$13/2^+$	−2.20(15)	−0.452(13)	0.12
^{203}Po	$5/2^-$	−2.56(15)	−0.425(13)	0.08
^{203m}Po	$13/2^+$	−3.43(15)	−0.352(13)	0.11
^{209}Po	$1/2^-$	−6.75(10)	−0.0813(10)	0.09
^{211}Po	$9/2^+$	−8.99(10)	0.104(10)	0.12

[a] The errors reflect only the experimental uncertainties. Systematic uncertainties arising from electronic factor and specific mass shift calculations of a magnitude similar to the experimental uncertainties should also be considered.
[b] Spin values from 11/2 to 15/2 have been proposed [32]. The isotope shift in the next column has been deduced assuming $11/2^+$, but this assumption does not influence the isotope shift extracted.
[c] Result of the fit with $B > 0$.
[d] Result of the fit with $B < 0$.

performed using the $6p^3 7s\ ^5S_2 \longrightarrow 6p^3 7p\ ^5P_2$ transition ($\lambda = 843.38$ nm, second excitation step, see Fig. 1). For this transition the position of the hyperfine structure (hfs) components $\nu_0^{F,F'}$ is determined by:

$$\nu_0^{F,F'} = \nu_0 - A\frac{K}{2} - B\frac{\frac{3}{4}K(K+1) - I(I+1)J(J+1)}{2(2I-1)(2J-1)IJ} + A'\frac{K'}{2} + B'\frac{\frac{3}{4}K'(K'+1) - I(I+1)J'(J'+1)}{2(2I-1)(2J'-1)IJ'}, \quad (1)$$

where ν_0 is the position of the centre of gravity of the hyperfine structure, $K = F(F+1) - I(I+1) - J(J+1)$, F is the total angular momentum of the atom ($\mathbf{F} = \mathbf{I} + \mathbf{J}$), A and B are the magnetic dipole and electric quadrupole hyperfine coupling constants respectively. The prime symbol denotes the upper level of the transition.

The experimental optical spectra were fitted with a convolution of a Gaussian Doppler profile, corresponding to the ion source temperature, and a deformed Lorentzian profile representing the laser lineshape. For more details see Refs. [25,26]. The parameters ν_0, A and B were varied during the fit, the ratios A'/A and B'/B were fixed. More details on evaluation of the A'/A and B'/B ratios will be given in the forthcoming article on the polonium electromagnetic moments [33]. To take into account the saturation of transitions, pumping processes between hyperfine structure (hfs) components and a population redistribution of the hfs levels the number of photoions for each frequency step was calculated by solving the rate equations for the given photoionization scheme (a similar method is described in details in Ref. [34]). The isotopic change of the charge radius $\delta\langle r^2\rangle_{A,A'}$ was evaluated in the same way as in our previous work [26].

While the spins of $^{203-211}$Po are known (see Table 1), the spins of $^{191-197}$Po are not confirmed experimentally. The tentative values

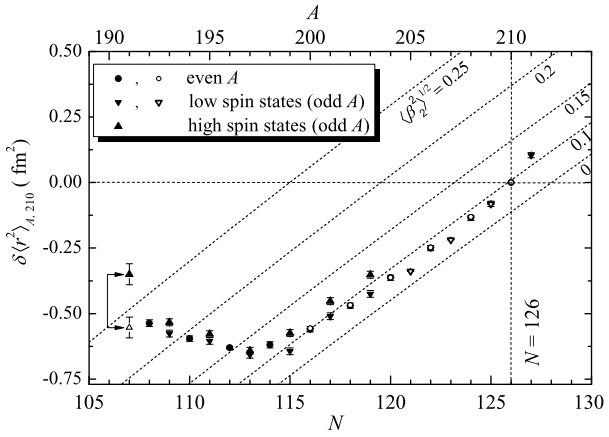

Fig. 5. Changes in mean-square charge radii for the polonium isotopes compared with the predictions of the droplet model [35] for various deformations. The data were normalized by using $\langle\beta_2^2\rangle_{208}^{1/2}=0.086$, evaluated from the energy of the first excited 2^+ state in ^{208}Po [36]. Our data (including data from Ref. [26]) are shown with filled symbols. Recalculated (by using King plot) charge radii based on isotope shifts from Ref. [23] are shown with open symbols. For ^{191}Po results of the fits with $B>0$ and $B<0$ are shown with the filled and opened up-triangles, respectively.

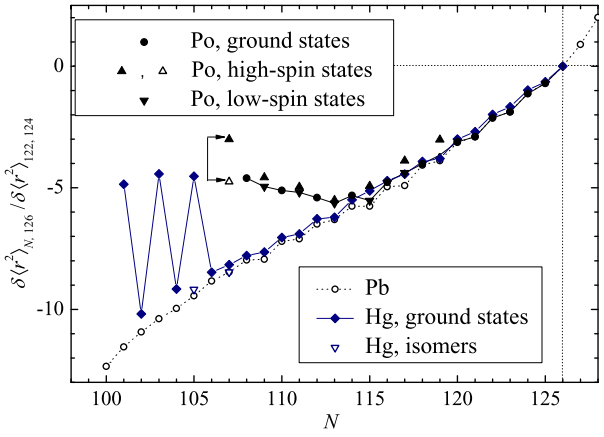

Fig. 6. Relative $\langle r^2\rangle$ for the even-Z $_{80}$Hg [38], $_{82}$Pb [24,39] and $_{84}$Po (this work and Refs. [23,26]).

quoted in the literature are based on systematics of hindrance factor values from α-decay studies. For the polonium isotopes with $A>195$, based on the number of observed hfs components (see Fig. 3), we can exclude $I=1/2$ for low-spin states. Obtained hfs spectra of the low-spin states of ^{193,195}Po can be equally well-fitted with $I=1/2$ or $I=3/2$. However, the isotope shift deduced from the fit has little sensitivity to the nuclear spin. Assuming a spin 1/2 or 3/2 for ^{195ls}Po gives a difference in the isotope shift less than 5 MHz while the statistical error is 150 MHz. The same is true for the high-spin state: the spectra of high-spin state ^{193hs}Po were fitted with spin values ranging from 13/2 to 9/2 yielding isotope shift values of $-1.11(15)$ to $-1.09(15)$ GHz respectively, thus identical within quoted uncertainties.

For the α-decaying polonium isotopes with $A\geqslant 193$, the decay of the high-spin and low-spin isomeric states towards their respective counterparts in the lead daughter nuclei is only hindered by a factor between 1.9 and 2.6 and can be considered as favoured α-decays according to the classification given in Ref. [37]. However, in contrast to the heavier polonium isotopes, the α-decay from the high-spin isomer of ^{191}Po towards spherical $13/2^+$ state in ^{187}Pb is hindered by a factor of 30 [18]. In the original paper [18], it was concluded that the α-transition between high-spin isomers was a strongly hindered $\Delta I=0$ transition and a spin $13/2^+$ was proposed for ^{191hs}Po. The strong hindrance was assumed to be caused by a difference in configuration between mother and daughter nuclei giving rise to a large difference in deformation between the ground and isomeric states in ^{191}Po, a phenomena similar to what was observed in the lightest mercury isotopes. A subsequent combined in-beam and decay study performed by the same group, however, did not firmly fix the spin of the ^{191hs}Po and a range from $11/2^+$ to $15/2^+$ was proposed [32]. It was nonetheless concluded that a large change of deformation occurred in ^{191}Po. We stress that the spin assumption does not strongly influence the extracted isotope shift: the isotope shifts extracted for $I=9/2$ or 13/2 for ^{191hs}Po differ less than the quoted uncertainty values. However, because of the low statistics obtained for the ^{191hs}Po data, an ambiguity exists with respect to the sign of the electric quadrupole hyperfine coupling parameter B. The data can be equally well-fitted with a positive or a negative B-parameter. Both fits are shown in Fig. 4 and resulting values are shown in Fig. 5 and Table 1. A full discussion on the final spin and parity assignments will be subject of a forthcoming paper where also the magnetic and quadrupole moments extracted from the present experiment will be discussed [33].

The isotope shifts and the deduced values of the mean-square charge radii changes are reported in Table 1 along with the values of the deformation parameter β_2, which were estimated using the expression:

$$\langle r^2\rangle_A \approx \langle r^2\rangle_A^{sph}\left(1+\frac{5}{4\pi}\langle\beta_2^2\rangle_A\right), \tag{2}$$

where $\langle r^2\rangle_A^{sph}$ is the mean-square radius of a spherical nucleus with the same volume. For the evaluation of $\langle r^2\rangle_A^{sph}$, the droplet model with a revised parametrization (second parameters set) [35] was used. The charge radii variations for the polonium isotopes and the droplet-model predictions for various deformation values (see Eq. (2)) are shown in Fig. 5.

The charge radii of the polonium isotopes follow the spherical droplet-model predictions rather closely down to ^{200}Po ($N=116$). However, in the region $191\leqslant A\leqslant 199$ a gradually increasing deviation is observed. The same trend is also clearly seen in the behavior of the deformation parameters $\langle\beta_2^2\rangle^{1/2}$, deduced by using Eq. (2). For example, the deformation parameter $\langle\beta_2^2\rangle^{1/2}$ increases gradually from ~ 0.1 (^{201}Po) to ~ 0.2 (^{193}Po) and ~ 0.23–0.27 (^{191}Po).

The similarities and discrepancies between the different isotopic chains in the lead region can be elucidated by comparing relative changes in mean-square charge radii $\delta\langle r^2\rangle$ according to the formalism introduced in Ref. [40] and thoroughly described in Ref. [41]. The values of $\delta\langle r^2\rangle_{N,124}$ are normalized within each isotopic chain to $\delta\langle r^2\rangle_{122,124}$ in order to allow a comparison between the isotopic chains. Fig. 6 shows the relative changes in $\delta\langle r^2\rangle$ for the mercury, lead and polonium isotope chains. Comparing lead with mercury shows, with the exception of the large isomer shift of the most neutron-deficient mercury isotopes, a remarkably similar trend. The same is true for the polonium and lead isotopes between $N=126$ and $N=116$. However, the lighter even- and odd-A polonium isotopes depart drastically from the systematic trend of the heavier isotopes and show also a deviation compared to the lead and mercury isotopes and to the ground states of the platinum isotopes (the latter are not shown in Fig. 6). This clearly indicates a strong onset of collectivity for the lightest polonium at $N=114$, far earlier than for the mercury and platinum isotopic chain. Moreover, again in contrast to the mercury isotopic chain, where strong odd–even staggering is present (the ground states ($I=1/2$) of the odd-A isotopes with $N\leqslant 105$ are

strongly deformed, while the even-A isotopes and ^{185m}Hg isomer ($I = 13/2$) remain nearly spherical or weakly deformed), no strong odd–even staggering of the charge radii of the ground states of the polonium isotopes is observed and for the lighter odd-mass isotopes ($N < 114$), both the ground and isomeric state have similar charge radii that deviate strongly from sphericity. It therefore appears more likely that the strongly retarded α-decay of the high-spin isomer in ^{191}Po is due to a configuration *and* spin difference between the two connected states and that ^{191}Po is indeed a transitional nucleus between the heavier presumably oblate deformed ($A \geqslant 192$) and lighter more strongly deformed presumably prolate ($A \leqslant 190$) polonium isotopes [12,20,21]. The enhanced collectivity of the polonium isotopes ($Z = 84$) compared to the mercury ($Z = 80$) might be due to the filling of similar high-j single-particle orbitals for protons and neutrons ($82 \leqslant Z, N \leqslant 126$) by approaching $N = 104$. Further studies of the lighter radon and radium isotopes should be pursued to further clarify this issue.

In conclusion, isotope shifts for odd-A polonium isotopes have been measured for the isomers and ground states of $^{191–203,209,211}$Po. The extracted charge radii show a strong deviation from sphericity for both isomeric and ground states in the lightest polonium isotopes with $A = 197$ onwards. A comparison of the values of the relative $\delta\langle r^2\rangle$ with the isotones in the lead and mercury isotopic chain shows that when going from spherical nuclei in the neighbourhood of doubly magic ^{208}Pb towards very neutron-deficient isotopes, deformation sets in at a much earlier stage for the isotopes with extra protons above the $Z = 82$ closure compared to the isotones below $Z = 82$. In this sense, the concept of intruder-analog states that should give rise to similar properties of the intruder states of the mercury and polonium isotopes, as introduced in Refs. [42,43] does not appear to be valid in the lead region. Extracting the magnetic and quadrupole moments from the present data and comparisons with the available results from in-beam spectroscopy should shed more light to this particular problem and will be discussed in a separate paper.

Acknowledgements

We would like to thank the ISOLDE Collaboration for providing excellent beams and the GSI Target Group for manufacturing the carbon foils. This work was supported by FWO-Vlaanderen (Belgium), by GOA/2004/03 (BOF-KU Leuven), by the IUAP – Belgian State Belgian Science Policy – (BriX network P7/12), by a grant from the European Research Council (ERC-2011-AdG-291561-HELIOS) and by the European Commission within the Sixth Framework Programme through I3-EURONS (Contract RII3-CT-2004-506065), by the U.K. Science and Technology Facilities Council, by the FiDiPro programme of the Finnish Academy and by the Slovak Research and Development Agency (Contract No. APVV-0105-10).

References

[1] K. Heyde, et al., Phys. Rep. 102 (1983) 291.
[2] J. Wood, et al., Phys. Rep. 215 (1992) 101.
[3] A.N. Andreyev, et al., Nature 405 (2000) 430.
[4] R. Julin, et al., J. Phys. G 27 (2001) R109.
[5] K. Heyde, J.L. Wood, Rev. Mod. Phys. 83 (2011) 1467.
[6] F.R. May, et al., Phys. Lett. B 68 (1977) 113.
[7] P. Möller, et al., At. Data Nucl. Data Tables 59 (1995) 185.
[8] A.M. Oros, et al., Nucl. Phys. A 645 (1999) 107.
[9] Y. Shi, et al., Phys. Rev. C 82 (2010) 044314.
[10] N.A. Smirnova, et al., Phys. Lett. B 569 (2003).
[11] B. Sabbey, et al., Phys. Rev. C 75 (2007) 044305.
[12] K. Helariutta, et al., Phys. Rev. C 54 (1996) 2799.
[13] K. Van de Vel, et al., Phys. Rev. C 68 (2003) 054311.
[14] K. Van de Vel, et al., Eur. Phys. J. A 17 (2003) 167.
[15] T. Grahn, et al., Nucl. Phys. A 801 (83) (2008).
[16] J. Wauters, et al., Phys. Rev. C 47 (1993) 1447.
[17] N. Bijnens, et al., Phys. Rev. Lett. 75 (1995) 4571.
[18] A.N. Andreyev, et al., Phys. Rev. Lett. 82 (1999) 1819.
[19] T. Grahn, et al., Phys. Rev. Lett. 97 (2006) 062501.
[20] J. Wauters, et al., Phys. Rev. Lett. 72 (1994) 1329.
[21] D.R. Wiseman, et al., Eur. Phys. J. A 34 (2007) 275.
[22] A. Andreyev, et al., Phys. Rev. C 73 (2006) 044324.
[23] D. Kowalewska, et al., Phys. Rev. A 44 (1991) R1442.
[24] H. De Witte, et al., Phys. Rev. Lett. 98 (2007) 112502.
[25] M.D. Seliverstov, et al., Eur. Phys. J. A 41 (2009) 315.
[26] T.E. Cocolios, et al., Phys. Rev. Lett. 106 (2011) 052503.
[27] B. Jonson, A. Richter, Hyperf. Int. 129 (2000) 1.
[28] V.N. Fedosseev, et al., Nucl. Instr. Meth. B 266 (2008) 4378.
[29] T.E. Cocolios, et al., Nucl. Instr. Meth. B 266 (2008) 4403.
[30] A.N. Andreyev, et al., Phys. Rev. Lett. 105 (2010) 252502.
[31] T.E. Cocolios, et al., J. Phys. G 37 (2010) 125103.
[32] A.N. Andreyev, et al., Phys. Rev. C 66 (2002) 014313.
[33] M.D. Seliverstov, in preparation.
[34] H. Backe, et al., Hyperf. Int. 162 (2005) 3.
[35] D. Berdichevsky, F. Tondeur, Z. Phys. A 322 (1985) 141.
[36] S. Raman, et al., At. Data Nucl. Data Tables 78 (2001) 1.
[37] Nucl. Data Sheets 112 (1) (2011) viii.
[38] G. Ulm, et al., Z. Phys. A 325 (1986) 247.
[39] S.B. Dutta, et al., Z. Phys. A 341 (1991) 39.
[40] R.J. Hull, H.H. Stroke, Phys. Rev. 122 (1961) 1574.
[41] P. Campbell, et al., Phys. Lett. B 346 (1995) 21.
[42] K. Heyde, et al., Phys. Rev. C 46 (1992) 541.
[43] C. De Coster, et al., Phys. Rev. C 61 (2000) 067306.